Periodic systems as road traffic noise reducing devices: prototype and standardization

Sergio Castiñeira-Ibañez, Vicente Romero-García, Juan Vicente Sanchez-Perez, Lluis Miquel Garcia-Raffi

PERIODIC SYSTEMS AS ROAD TRAFFIC NOISE REDUCING DEVICES: PROTOTYPE AND STANDARDIZATION

Sergio Castiñeira-Ibáñez[1], Vicent Romero-García[2], Juan Vicente Sánchez-Pérez[3]*, Luis Miguel García-Raffi[4]

[1]Departamento de Física Aplicada, Universitat Politécnica de València, Valencia 46022, Spain
[2]Instituto de Investigación para la Gestión Integrada de zonas Costeras,Universitat Politécnica de València, Paranimf 1, 46730 Gandia, Spain
[3]Centro de Tecnologías Físicas: Acústica, Materiales y Astrofísica, Universitat Politécnica de València, Valencia 46022, Spain
[4]Instituto Universitario de Matemática Pura y Aplicada, Universitat Politécnica de València, Valencia 46022, Spain

Abstract

The design, the realization of the prototype and the acoustic standardization process of a novel periodic system made up of multi-physical phenomena scatterers as a road traffic noise reducing device are reported in this work. The structure analysed here, inspired by Sonic Crystals, has been designed following the guidelines established in recent works according to the concept of tunability. Thus, the acoustic barrier proposed here includes several mechanisms of noise control, such as scattering, resonances and absorption, in such a way the range of frequencies where each mechanism works can be chosen in the design process. The constructive solutions taken into account in the manufacturing process of the device are also explained. On the other hand, as a road traffic noise reducing device, the system has been evaluated by the European standards. Finally, due to the fact that this device is made up of separated scatterers, an advantage in the reduction of the resistance to wind is observed in a wind tunnel experiment. The results of all these analyses allow us to present a novel type of road traffic noise reducing device with interesting alternative properties with respect to the classical acoustic barriers.

Key words: acoustic barrier, environmental solutions, road traffic noise control, sonic crystals

1. Introduction

Environmental noise, defined as an unwanted or unpleasant outdoor sound generated by transport and industry, is one of the main local environmental problems in the countries of the European Union (EC Directive, 2002), but generally speaking it is a problem of the industrialized countries. Traditionally noise has been linked with some health problems such as annoyance and speech interference, fatigue, sleep disturbance, cardiovascular disorders or some reduction in the performance at work or school (Kotzen and English, 1999; Platon and Hionis, 2014).

One of the classical methods to reduce the environmental noise levels in its transmission is the use of acoustic barriers (ABs). These barriers can be defined as solid systems built between the source of noise and the receiver. The acoustic mechanism involved here is simple: the interposed object reduces the noise level through several mechanisms such as absorbing, reflecting sound waves or forcing them to take a path over and around the barrier that is longer than the direct one. This last mechanism, called diffraction, can be considered as one of the main factors that decreases the effectiveness of the barriers (Harris, 1991; Kotzen and English, 1999) (Fig. 1). ABs should be designed and constructed in such a way so that they can reduce the loudness of road traffic noise by as much as half, although they do not completely block all road traffic noise, can be

* Author to whom all correspondence should be addressed: e-mail: jusanc@fis.upv.es; Phone: +34 963877523

effective regardless the material used, they should be tall and long without openings -excluding those due to security reasons- and they should be visually appealing and preserve aesthetic values (FHWA U.S.A., 2011). But the reality is that ABs do not completely block the noise and their design presents serious aesthetic problems to deal with a solid and continuous barrier lodged between source and receiver (FHWA U.S.A., 2011). On the other hand, another factor to take into account is the heavy load generated by the force of the wind, resulting in a large volume of foundations, especially for large barrier heights.

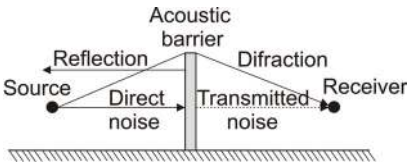

Fig. 1. Scheme of the acoustic performance of an AB

One of the main research lines in the field of this classical ABs is focused on reducing the effect of the diffraction over the top edge. Efficiency of ABs has been increased by designing new profiles far away from the simple edge of the classical ones (Mak and Leung, 2013; Okubo and Fujiwara, 1999; Watts, 1996; Watts and al., 2004). This fact has led to a stalemate in the technological development of the classical ABs.

In this paper we report the design, the manufacturing, the acoustic standardization in accordance with European standards, and the analysis of the structural efforts of a novel wideband road traffic noise reducing device with that of classical ABs. This novel barrier is formed by a periodic distribution of cylindrical multi-physical phenomena scatterers, based on the well-known Sonic Crystals (SC) (Martínez-Sala et al., 1995; Sánchez-Pérez et al., 1998) that, in comparison with the classical ABs, includes another physical mechanism to control the transmission of acoustic waves based on Bragg interferences due to a multiple scattering (MS) process (Chen and Ye, 2001), as we will explain in Section 2.

The design process has been developed in accordance with the method proposed by some of us in which the concept of tunability is presented (Romero-Garcia et al., 2011). Thus, apart from the phenomenon due to the existence of an array of scatterers, other noise control features using the local acoustical properties of the scatterers, such as resonances or absorption, have been introduced. Therefore, several mechanisms of noise control are involved in these systems in conjunction with the Bragg phenomenon without disturbing it, providing a high technological procedure to the industrial field of the ABs. The complete manufacturing process is also explained, including the materials used and the constructive solutions adopted. Also, the standardization tests usually applied to classical road traffic noise reducing devices are used to acoustically characterize this SC barrier. Although these tests are not designed to evaluate this kind of barrier, the obtained results are promising, showing that SC barriers can compete with the traditional ones under the acoustical point of view. Finally, a comparison between the wind load supported by both the developed device and a classical AB formed by a wall is done, as the size of their foundations or the efforts transmitted to the ground depends basically on this kind of load. This last study can help us to propose some specific applications of the new device.

The paper is organized as follows: In section 2 we develop a brief introduction to SC, explaining their transmission properties and the theoretical design of this new type of AB. In section 3 we present the constructive characteristics of the prototype as well as the acoustic characteristics of the materials used. The acoustic standardization for road traffic noise of the constructed prototype is developed in section 4. In section 5 we present the structural efforts analysis carried out in a wind tunnel. Finally, section 6 summarizes the main results of the work.

2. Design of the prototype: Sonic Crystals as acoustic barriers

Since the beginning of the 90´s the study of the propagation of electromagnetic waves in a medium with periodic modulation of its dielectric properties has attracted increasing interest (John, 1987; Yablonovitch, 1987). One of the most interesting properties of these systems is the existence of ranges of frequencies, related with the periodicity of the medium, where the propagation of waves is forbidden. These ranges of frequencies were called band gaps (BG) due to the analogy with semiconductor crystals, and the underlying physical mechanism is the Bragg interference.

A few years later, the analogy to the case of elastic waves was investigated and determined by several theoretical works (Kushwaha et al., 1993; Sigalas and Economou, 1992), and the resulting structures were called Phononic Crystals (PC). These periodic structures, which present BG for elastic waves, are formed by periodic arrays of elastic scatterers embedded in a different elastic and isotropic background. If one of the components of the composite (scatterers or background) is a fluid medium the resulting structures are called SC. One of first examples of SC is given by a minimalist sculpture made of steel cylinders in air (Martínez-Sala et al., 1995) that was used to experimentally show for the first time the existence of BG in periodic structures. The possibility to manipulate airborne sound by means of SC motivated the idea of designing acoustic barriers based on these structures (Romero-Garcia et al., 2011; Sánchez-Pérez et al., 2002).

2.1. Acoustic barriers based on first generation sonic crystals

The first acoustic barriers based on SC were theoretically proposed by Kushwaha (1997) and later were designed, developed and constructed at the beginning of this century (Sánchez-Pérez et al., 2002). In this AB based on first generation SC the mechanism of noise control was the Bragg interferences, i.e. the attenuation mechanism due to the periodicity of the structure. This system was made of rigid scatterers embedded in air. Fig. 2a shows a prototype, placed at the Universitat Politècnica de València, formed by a triangular arrangement of 3 m long PVC cylindrical pipes. The complete structure is formed by 198 cylinders located in 6 rows of 33 elements, occupying an area of 7.2x1.1m^2.

The acoustical attenuation properties of this barrier, shown in Fig. 2b, are represented by its attenuation spectrum in the chosen range of frequencies (0-2000 Hz), characterized by means of the Insertion Loss (IL), defined as the difference between the sound pressure levels recorded at the same point without (direct measurement) and with (interfered measurement) the sample (Eq. 1):

$$IL = 20\log_{10}\left(\frac{|P_{direct}|}{|P_{inter}|}\right)dB \qquad (1)$$

In Fig. 2b one can see the differences in both the size and the position of the BG for the previous structure for two angles of incidence of the wave (0º-30º). Moreover, Fig. 2b shows the first and second attenuation bands related to the first and the second BG due to the periodicity for 0º of incidence (black continuous line) centred at 772 Hz (first BG) and 1500 Hz (second BG). It is worth noting that inside the BG the attenuation obtained by the SC can compete with the attenuation of a classical AB although out of the first and second BG the attenuation is significantly decreased.

Efficient ABs should attenuate sound in all directions and in the complete range of frequencies. However, for the case of SC, the distance between the scatterers or the angle of incidence of the wave on the structure determines the range of frequencies of the BG, and the diameter of the cylinders determines the width of frequencies occupied by BG. Then, the use of the Bragg interferences as the unique mechanism of noise control is not enough to design efficient ABs based on SC.

To avoid these problems and also to increase the attenuation properties of the SC, a second generation of arrays of multi-physical phenomena cylinders has been developed. In them, more mechanisms of noise control are added to SC. This new generation allows the design of specific ABs for specific noise problems, as we will see in the following Section.

2.2. Acoustic barriers based on second generation sonic crystals

2.2.1. Theoretical tools for the design of second generation SC acoustic barriers

Due to the geometric shape of the designed scatterers and the different physical mechanisms involved in its design, the Finite Element Method (FEM) seems a good theoretical tool to design this kind of ABs. Using FEM and considering temporal harmonic dependence, we have studied the propagation of sound described by the Eq. 2:

$$\frac{1}{\rho c^2}\frac{\partial^2 p}{\partial t^2} = \nabla\left(\frac{1}{\rho}\nabla p\right) \qquad (2)$$

The main characteristics of the simulations are: (i) The pressure acoustic module belonging to the commercial software COMSOL 3.5a is used in this work to obtain the numerical predictions; (ii) Due to the characteristics of the numerical method, we have designed the structure of the barrier first and then we have obtained with COMSOL the solutions by numerically solving Eq. 2 at each point of the selected domain, taking into account every acoustic effect included, such as resonances or absorptions. Thus, the resonances arise by themselves by the geometry of the scatterers and the absorption characteristics must be included in the model as we will explain later.

In the entire process we have calculated the IL of a transversal section of the barrier as an index to evaluate the attenuation properties of the proposed AB. An example of the numerical solution carried out can be observed in Fig. 3. In this Figure, two pressure maps are represented at 310 Hz and 810 Hz. Note the resonance effect inside the cylinders (Fig. 3a) and the attenuation due to the first Bragg´s frequency (Fig. 3b) in the shadow zone.

A detailed description of the specific method used here as well as its theoretical and experimental validation can be found in previous articles (Romero-Garcia et al., 2011); (iii) A plane wave travelling from left to right has been considered throughout the simulations and the IL has been calculated at a testing point placed behind the structure in the symmetry axis, in the middle of the barrier and 1m away from it, using Eq. 1.

The IL spectrum can be seen in Fig. 4b; (iv) The solution domain has been discretized using 75.522 elements; (v) To simulate the characteristics of our problem, we have considered that the wave propagation occurs in free space conditions (unbounded acoustic domain). This assumption is known as the Sommerfeld condition.

However, for our case in which we solve the problem numerically using FEM, some artificial boundaries should be considered in the numerical domain. We have used here the perfectly matched layers (PML) to simulate this condition.

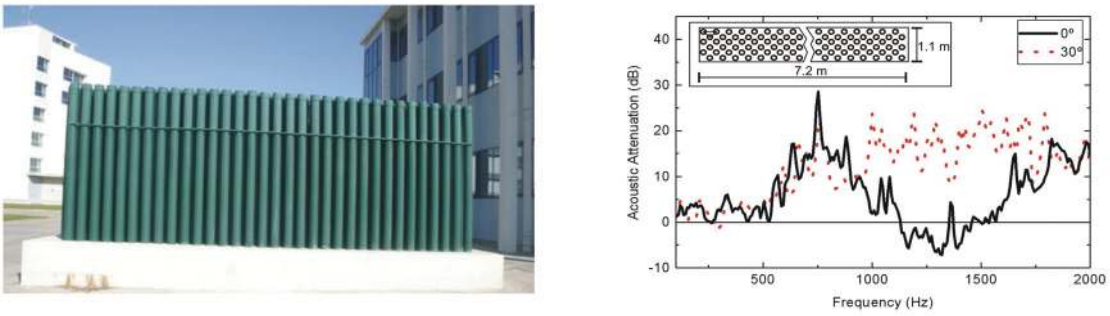

(a) **(b)**

Fig. 2. Some characteristics of an AB based on first generation SC; (a) Picture of a first generation SC acoustic barrier; (b) Experimental IL spectra for the ABs shown in (a). The results have been obtained in a point located at 2 m from the barrier and 2 m above the ground. Continuous (dotted) lines represent the IL at 0º (30º) of incidence

(a) **(b)**

Fig. 3. Numerical IL pressure maps obtained in the design process. (a) 310 Hz. One of the resonances inside the small cylinders is shown as a reinforcement of the acoustic pressure; (b) 810 Hz (Bragg´s frequency). The attenuation due to the effect of isolated scatterers can be seen in the map; the considered domain and the section of the barrier designed are also shown in both maps

This method was presented by Berenger (1994) and is useful to emulate the Sommerfeld condition in the numerical solution of scattering and wave radiation problems. Basically, the PML method consists of a coordinate transformation (Liu, 1999). This transformation is a scaling to complex coordinates so that the new medium becomes selectively dissipative in the direction perpendicular to the interface between the PML and the physical domain.

Although in practice the external boundary of the PML produces artificial reflections because the PML has to be truncated at a finite distance from the domain of interest, from the numerical point of view these reflections have minor importance due to the exponential decay of the acoustic waves inside the PML.

As an example, it has been proven that, for Helmholtz-type scattering problems, the approximate solution obtained using the PML method exponentially converges to the exact solution in the computational domain as the thickness of the layer goes to infinity (Lassas and Somersalo, 1998). (vi) The different parts of the barrier have been modelled using the Neumann boundary condition for the rigid materials and the Delany-Bazley model for the absorbent material (rockwool), characterized by its flow resistivity $\sigma = 23.000\, kg/m^3 s$.

2.2.2. Results of the design process

Using the numerical tool described above, we have designed a novel AB based on SC made of solid resonant and absorbent cylindrical scatterers embedded in air.This type of AB is protected under Spanish patents (Sánchez-Pérez et al., 2003, 2009). The system uses several noise control mechanisms and they can be designed in such a way the attenuation bands obtained by each of the mechanisms involved acts in a previously determined range of frequencies.

In this section, we present only the design process of the AB based on the numerical simulations done. To do that, we have followed the design method developed by some of us based on the concept of tunability (Romero-García et al., 2011). This method has been already used to design AB based on SC. The conclusions obtained here provide the guidelines to construct the prototype to standardize this type of barrier, although we base our decision only on the numerical results obtained here. Apart from the BG due to the periodicity of the structure, we can introduce additional physical properties in each one of the scatterers to control the attenuation capabilities of the system. Thus, the cylinders are made of a combination of rigid and absorbent materials with a geometrical shape that contains resonant cavities. The designed scatterers

are based on the concept of split ring resonator (SRR) (Hu and Chan, 2005). Fig. 4a shows the transversal section of the designed scatterer. A cylindrical rigid wall is covered by a porous material (rock wool with 100 kg/m^3 density and flow resistivity $\sigma = 23.000\ kg/m^3 s$).

A slit is made all along the cylinder in such a way the shape of the scatterer presents a resonant cavity. The walls of the inner core can be considered acoustically rigid. In the proposed SC, the existence of absorbent material in each scatterer gives a baseline of noise attenuation, and the resonant cavities produce attenuation peaks due to the resonances. Resonant frequencies mainly depend on the volume of the resonators. Then we have used cylinders with two different diameters for adding two resonance peaks placed at different ranges of frequencies of the spectrum.

The multi-physical phenomena scatterers are arranged in a triangular array with a separation between the scatterers equal to 0.28m, as can be seen in the inset of Fig. 4b. The attenuation effects of this design can be seen in Fig. 4b. One can observe the existence of the different attenuation peaks due to the different mechanisms considered. Thus, the attenuation peaks (1) and (2) are both due to the resonances corresponding to the two sizes of the cavities of the scatterers considered. The attenuation peaks (3) and (4) correspond to the Bragg interferences on the array. Finally, the continuous attenuation level that appears from 500 Hz onwards corresponds to the effect of the absorbent used in every cylinder of the structure. To evaluate the acoustic response of the designed AB, we have included in Fig. 4b the theoretical attenuation level for a classical AB with the same height and width using the Maekawa´s method (Maekawa, 1968). The increase in the attenuation in most of the analyzed frequencies can be seen.

3. Materials and construction of the device

Once the different elements of the AB have been designed, the next step is the realization of the prototype to standardize its acoustical response, following the design characteristics of the different parts of the structure obtained in the previous section.

To do that, two considerations are needed to construct the sample: (i) the choice of the suitable materials, from the sound attenuation point of view, that form the device and (ii) the design of the anchorage of the scatterers to the base of the barrier. We have used three types of materials to manufacture the scatterers:

- Hard core: Constructively, the hard core serves as structural support for the scatterers, its interior is an acoustic resonant cavity and its exterior contributes to the Bragg interferences phenomenon that appears when all the scatterers are placed periodically. The chosen material is iron due to its good construction characteristics and also because it presents the appropriate reflecting properties under the acoustical point of view. The specific geometrical characteristics of the two iron cylinders used as internal hard cores are: external diameter 165 mm (114 mm) and 4.85 mm (4.5 mm) thickness respectively. The cylinders are slotted along its entire length with a size of slot, *L*, equal to 20 mm.

- Absorbent material: The role of this layer is to absorb the acoustic waves, and it is placed in such a way as to cover the hard core. We have chosen rock wool with 100 kg/m^3 density, which has the necessary consistence to be installed in outdoor conditions together with an optimum acoustic absorbent capability. According to the size of the hard cores, two different internal diameters have been used, 114 mm and 169 mm, with the thickness being equal to 40 mm.

- Perforated Plate: This element does not play a structural role but protects the rock wool to the environment and it has a minimum influence in the scattering process. This preserves the acoustical performance of both the hard core and the absorbent material. Moreover, the degree of perforation of this external covering has been chosen to preserve the attenuation properties of the rock wool cover. We have used an iron perforated plate of 1 mm thickness and perforations of 5 mm of diameter. The percentage of perforation is around 51%.

On the other hand, the design of the base where the scatterers are placed is as follows: Two iron sheets (3 mm thickness) have been perforated with the placement pattern of the scatterers using laser techniques.

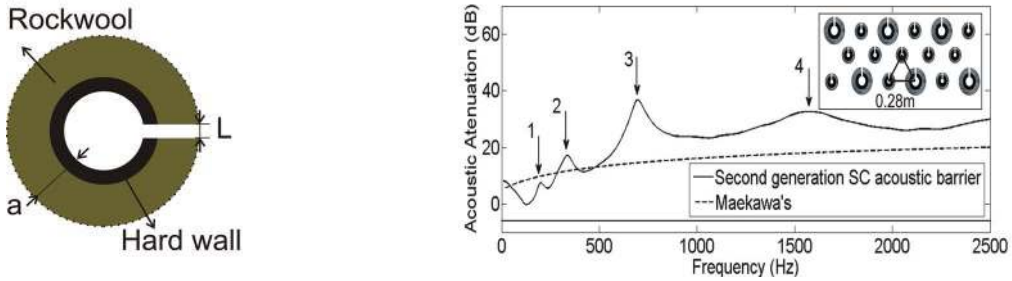

(a) **(b)**

Fig. 4. Design and acoustic characteristics of the AB proposed; (a) Transversal section of the designed scatterer; (b) IL spectrum in the measurement point defined in the previous section simulated by means of FEM The inset shows transversal view of the analyzed array

Then, both sheets have been placed one above the other with a separation of 200 mm distance in such a way that each hard core of any of the cylinders crosses both plates. This results in a perfect vertical position of the scatterers.

Several iron bars are disposed vertically between the two sheets to tie the complete structure and avoid deformations on the upper part due to the weight of the scatterers. To construct the device we have distributed 14 multi-physical phenomena cylinders with 247 mm of external diameter and 28 of 196 mm of external diameter. The total surface occupied by the sample is 4,00x0,76 m^2, and the height of the scatterers is 3 m. Fig. 5 shows different steps in the manufacturing of the device.

Also in Fig. 5c one can see the acoustic behaviour of the different elements of the scatterers. The experimental IL spectra for each one of the elements which form the scatterers have been measured in an anechoic chamber to avoid undesirable acoustic effects such as reflections on the walls. Moreover, one can observe the acoustic transparency of the perforated plate in the range of the analyzed frequencies. In the inset one can observe the first two resonance peaks of the biggest hard core (around 300 Hz and 600 Hz).

Finally, the IL of the active acoustic elements (hard core plus absorbent) can be seen. It is worth noting that in this last case the presence of the resonance peaks works constructively with the baseline of the absorbent in the total acoustic response of the complete scatterer.

4. Acoustic standardization

In order to acoustically characterize the second generation AB based on SC, we have carried out two acoustic tests in a laboratory approved for this purpose. Selected tests are used to characterize ABs for road traffic noise according to the European standard. In particular, the standards EN 1793: 1997 relative to road traffic noise reducing devices, test the method for determining the acoustic performance: Part 1: Intrinsic characteristics of sound absorption (CEN, 1997a), Part 2: Intrinsic characteristics of airborne sound insulation (CEN, 1997b), and Part 3: Normalized road traffic noise spectrum (CEN, 1997c), have been used to characterize our barrier.

The first two standards define the tests that have been made, relative to the noise absorption and their behaviour with regard to the spread of airborne noise, while the third one defines the normalized road traffic noise spectrum, which is used as a reference to obtain a ranking of barriers on the basis of their acoustic characteristics. In the following, we briefly describe these standards, as well as the results obtained by our barrier in each one of the tests.

4.1. Test 1: Intrinsic characteristics of sound absorption: EN-1793-1:1997

The goal of this test is to obtain the evaluation index of the acoustic absorption (DL_α) through experimental measurements in a reverberant chamber, evaluating the results according to the standard.

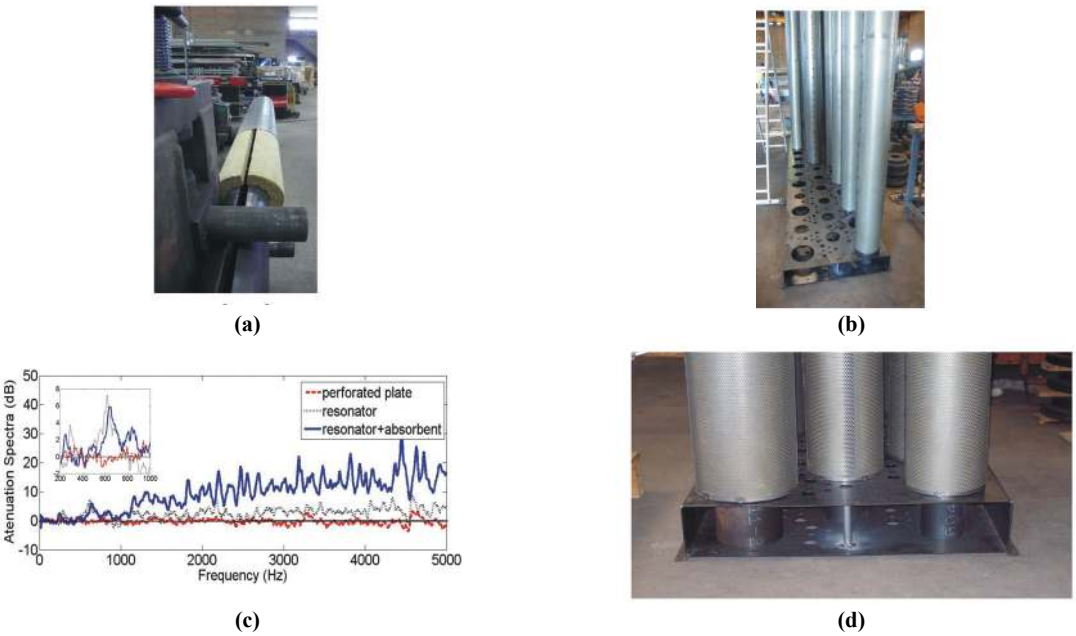

Fig. 5. Different steps in the manufacturing process of the ABs based on second generation SC used in the standardization process; (a) Assembly of the three elements of the scatterers (hard core, absorbent and perforated plate); (b) Anchorage system of the scatterers in the base structure (c) IL spectra of the different materials and combinations measured in the anechoic chamber; (d) Constructive detail of the fastening system showing the assembly between the bottom of the scatterers and the basis

We have used the ISO (2003), to determine the test procedure, and ISO (1997) to evaluate the results and to classify the performance of the barrier.

According to the standard CEN (1997a), a real model of the barrier is located next to one of the walls of the reverberant chamber. Five microphones and two sound sources are placed in front of the device as one can see in Fig. 6. Pink noise is used throughout the test. The reverberation times as a function of the frequency are obtained for each third octave band in the range from 100 Hz to 5000 Hz. Then, the equivalent absorption area (A_t) for each third octave band is calculated by using Sabine´s equation (Eq. 3):

$$A_t = A_2 - A_1 = 55.3V\left(\frac{1}{c_2 t_2} - \frac{1}{c_1 t_1}\right) - 4V(m_2 - m_1) \quad (3)$$

where: c is the sound propagation velocities in air for the temperature T; V is the volume of the empty reverberant chamber; t is the reverberation time of the chamber which varies with the frequency and m is the sound absorption coefficients for the reverberant chamber, calculated according to the standard ISO (1993) taking into account the climatic conditions of the chamber during the measurement. Subindexes 1 and 2 correspond to the situation with and without the sample respectively.

The next step is to obtain the sound absorption coefficient (α_S), again dependent on the frequency, according to the expression (Eq. 4)

$$\alpha_S = A_t / S \quad (4)$$

where: S is the total surface of the barrier.

Finally, and following the standard CEN (1997a), DL_α is calculated using Eq. 5:

$$DL_\alpha = -10\log\left|1 - \frac{\sum_{i=1}^{18} \alpha_{S_i} 10^{0.1L_i}}{\sum_{i=1}^{18} 10^{0.1L_i}}\right| \text{ (dB)} \quad (5)$$

where: L_i represents the sound level for each third octave band of the normalized road traffic noise spectrum (dB) given by the standard CEN (1997c).

The value of this index is used to classify the barrier with regard to its acoustic absorption characteristics. In our case, DL_α=8dB, which corresponds to the A3 category that is in accordance with the European standard EN-1793-1:1997, in the second level regarding its acoustic absorption characteristics.

This result shows that a non continuous noise barrier formed by multi-physical phenomena cylinders can compete, from the acoustic point of view, with traditional ABs formed by continuous systems. Fig. 6 also shows the variation of α_S as a function of the frequency and the classification of the barriers under the absorption point of view, which appears in the standard used.

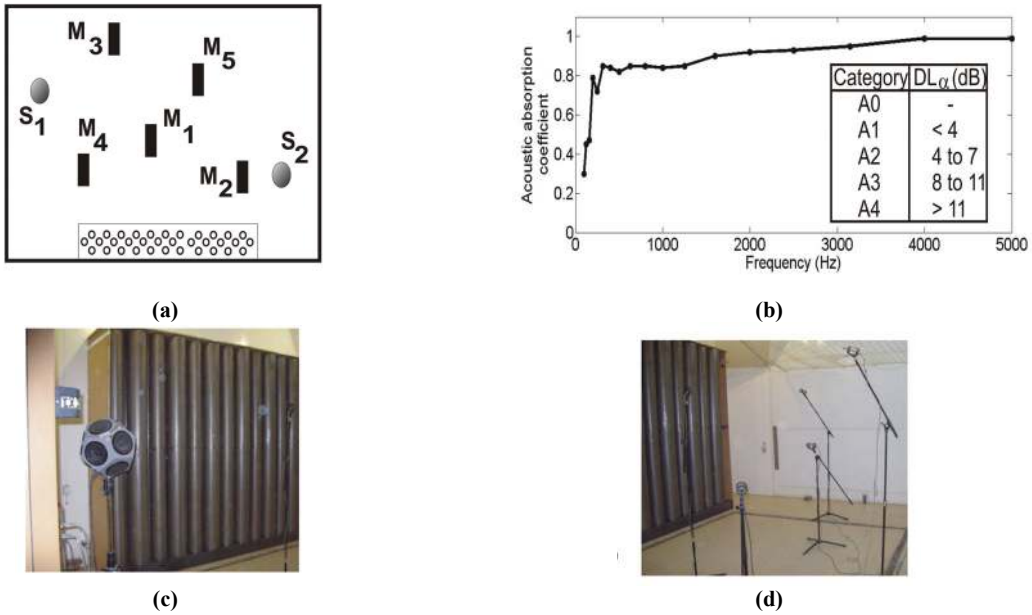

Fig. 6. Sound absorption standardization; (a) Scheme of the arrangement of the two sources (S_1 and S_2) and five microphones (M_1 to M_5) used for the characterization in the reverberant chamber; (b) Variation of α_S as a function of the frequency in the chosen range of frequencies (octave bands). The classification of the barriers as a function of DL_α can be seen in the inset; (c) and (d) Details of the arrangements of microphones, sources and sample in the reverberant chamber

4.2. Part 2: Intrinsic characteristics of airborne sound insulation: EN 1793-2: 1997

The second test checks the intrinsic characteristics of the barrier relative to the airborne sound insulation. The details of the test are indicated in the standard CEN (1997c). To do that, the evaluation index of the airborne sound insulation DL_R (dB) is calculated according to the standard ISO (2010).

This test is performed in a transmission chamber, in such a way the sample is located in the middle, dividing the chamber into two parts. In one part, called the emission chamber, a pressure sound level is generated so that in the other part of the chamber, which is called the receiving chamber, the sound level is 15 dB higher than the background noise in every frequency band from 110 Hz to 5000 Hz.

The noise level is measured in the emission chamber in these conditions. Some details of the experimental set up can be seen in Fig. 7. Then the process is repeated, with the measuring being done in this case in the receiving chamber. From these two levels, the difference of levels D can be achieved (Eq. 6):

$$D = L_1 - L_2 \tag{6}$$

where: L_1 and L_2 are the average sound pressure level (dB) in the emission and the reception chambers respectively. D must be corrected using a factor that depends on the reverberation time, on the volume of the reception chamber and on the common surface of separation between the two chambers. Thus, the acoustic reduction index R is (Eq. 7):

$$R = L_1 - L_2 + 10\log\left(\frac{St}{0.163V}\right) \tag{7}$$

where: S is the surface of the sample and t and V are the reverberation time and the volume of the reception chamber respectively.

The variation of R as a function of the frequency is shown in Fig. 7b. Finally, DL_R is calculated using the following expression (Eq. 8):

$$DL_R = -10\log\left|\frac{\sum_{i=1}^{18} 10^{0,1L_i} 10^{0,1R_i}}{\sum_{i=1}^{18} 10^{0,1L_i}}\right| \text{ (dB)} \tag{8}$$

where: L_i is the sound level for each third octave band of the normalized road traffic noise spectrum given by the standard CEN (1997c).

The value of this index enables us to classify the capability of airborne sound insulation of the checked barrier. In this case, DL_R=20dB, which corresponds to the category B2 specified in the standard CEN (1997b).

5. Determination of the structural efforts: wind tunnel

One of the main structural problems of the ABs is related with the efforts that are transmitted to the ground due to the different systems of loads supported by the structure.

Indeed, as the classical ABs are continuous systems, the transmitted efforts due to the wind are important and generally grow with the height of the barrier, as Luo and Yang (2010) demonstrated for the case of a high speed train moving on a viaduct, increasing the volume of foundations.

Thus, the cost of the product can be both technically and economically expensive, making their placement difficult in certain places. However, the ABs based on SC are formed by periodically distributing multi-physical phenomena scatterers, and this fact allows the wind to pass through, decreasing the efforts that are transmitted to the structure where the AB is located.

To estimate the values of these efforts in our barrier and to compare them with those corresponding to a classical barrier, we have carried out some laboratory experiments in a wind tunnel with dimensions 2.14 m high, 1.8 m wide and 12 m long, using the following protocol.

First, we have designed and constructed two models in a scale 1:5 for both a classical barrier and a SC barrier. This scale has been chosen in such a way the height of the sample occupies only 1/3 of the height of the wind tunnel in order to avoid interactions of the walls of the tunnel with the flow of the contours.

The size of the models is given by the dimensions of the wind tunnel. Thus, the dimensions of the models are: 60 cm high, 2 cm wide and 100 cm long for the classical barrier and 60 cm high (on average), 20 cm wide and 100 cm long for the SC barrier. This last one is formed by three rows of hollow cylinders with different heights and diameters and with a slot along its entire length. In Fig. 8a one can see some details of both models.

Second, we have to consider the action of the wind on both ABs as it was generated by the atmospheric pressure field. According with the Spanish Technical Building Code (SMD, 2006), we have considered here a ground roughness corresponding to urban or industrial areas. To simulate these conditions, we have to prepare the Atmospheric Boundary Layer (ABL) inside the wind tunnel. Near the surface, the texture of the ground has a strong influence in the movement of the wind and the ABL takes into account this influence. In this region, atmospheric turbulences due to thermal or mechanical imbalances are produced, increasing the chaotic movements of the air.

In this test, we have simulated typical flow conditions, assuming an area with uniform vegetation or buildings.

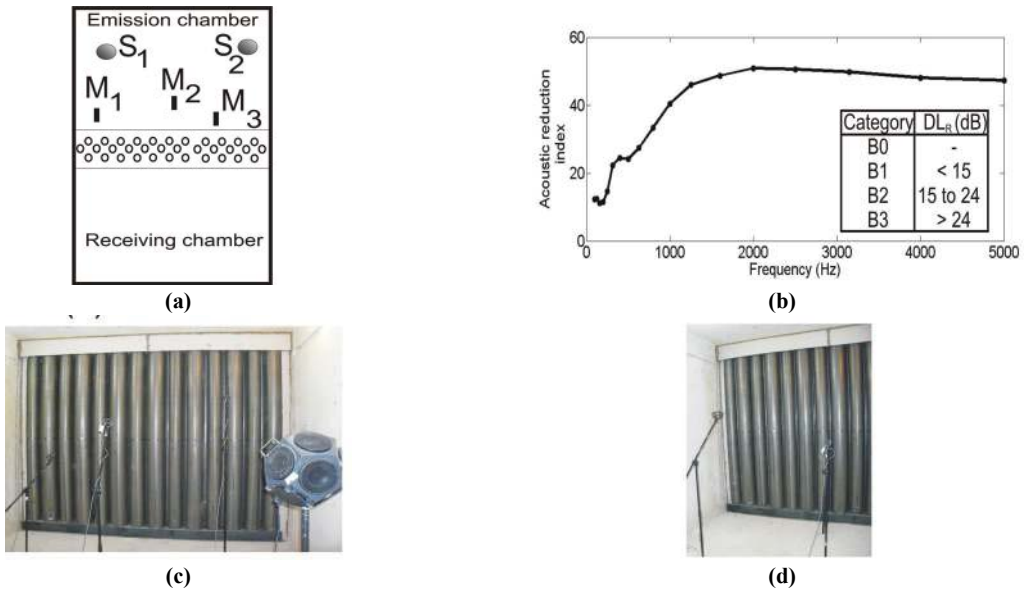

Fig. 7. Airborne sound insulation standardization; (a) Scheme of the experiments carried out in the transmission chamber; (b) Experimental values of the index *R*; (c) y (d) details of the experimental set up used to standardize the barrier under the point of view of its response to the airborne sound insulation

Fig. 8. Details of the set up used in the wind tunnel; (a) A view of the middle part of both the SC and the classical barriers. This part is located above the balance in order to measure the desired efforts; (b) Placement of the middle part on the balance inside the wind tunnel and (c) A view of the arrangement of obstacles inside the wind tunnel in order to simulate the ABL conditions. The SC barrier can be seen at the rear of the picture

To simulate the ABL profile, several obstacles with different shapes and sizes are located along the tunnel. Some details of the arrangement considered can be seen in Fig. 8c.

Third, we have prepared the experimental set up. To measure the wind efforts on the two different barriers we have used a precision balance AMTI MC 36 that allows the measurement of forces in the three directions of the space. In this case we are interested in measuring both the force in the wind direction and the corresponding overturning momentum on the bases of the barriers.

The knowledge about the variations of these efforts with the wind speed is necessary to determine the size of the foundations of the barrier. In Fig. 8b we show the set up used.

One can see that both types of barriers have been cut into three sections so that one of them, with the same width as the balance, is placed in the centre and above it.From these tests we have obtained the efforts on the model in real-time conditions. With these values and applying criteria of similarity and scale, we can obtain the values of the actions on the model.

Considering the experimental results, we propose the following second-degree polynomial expressions for the drag efforts of both the SC and the classical barriers (Eq. 9). In these expressions U is the wind speed.

$$\begin{aligned} F_{SC} &= 0.031U^2 - 0.025U - 4.7867, \\ F_{CB} &= 0.0578U^2 - 0.6433U + 2.84. \end{aligned} \tag{9}$$

Analogously, we propose the following second-degree polynomial expressions for the overturning momentum case (Eq. 10).

$$\begin{aligned} M_{SC} &= 0.0686U^2 - 0.0363U - 2.3493, \\ M_{CB} &= 0.1193U^2 - 0.8034U - 0.2399. \end{aligned} \tag{10}$$

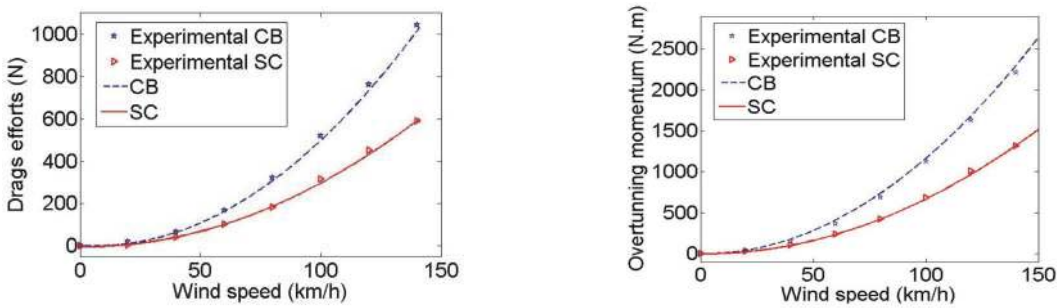

Fig. 9. Experimental and fitting results of the wind tunnel tests; (a) Variation of the drag effort and (b) Variation of the overturning momentum, as a function of the wind speed for both the Sonic Crystal (SC) barrier and the Classical barrier (CB)

The values of the correlation coefficients of the fitting curves are, in any case, 0.96. These values show the suitable fitting done considering second-degree polynomials curves. To calculate the percentage of the extra efforts supported by the Classical Barrier with respect to the SC barrier, we have calculated the area enclosed by the effort curves and the X axis (wind speed) for both the drag efforts and the overturning momentum.

Taking into account the obtained results one can conclude that the SC barrier supports efforts considerably smaller than the classical barrier, with this reduction on average being around 42% for both the drag efforts in the wind direction and the overturning momentum.

6. Conclusions

The acoustical and the structural performances of a new type of acoustic barrier for airborne sound, called by us Second Generation Sonic Crystal Acoustic Barrier, have been examined in this paper. The barrier is formed by a triangular arrangement of multi-physical phenomena cylindrical scatterers with different diameters and types of materials.

From the point of view of acoustics, the different steps in the design and the construction of the prototype have been explained using numerical tools and experimental results obtained in the laboratory. Bragg interferences, absorption and resonances are the three mechanisms of sound attenuation involved in the acoustic response of the barrier.

The results of the acoustic standardization, related to the absorption and the airborne sound insulation, show the tunability of the attenuation capabilities for the SC barrier, being competitive with respect to the classical ones formed by walls. One of the main characteristics of this type of barrier is the fact that they enable the design to be according to the type of noise that is needed to be controlled, therefore introducing therefore an important technological factor in the field of the acoustic barriers. This tunability is a consequence of the constructive interaction of the different mechanisms of sound attenuation involved in such a way that it is possible to select the range of frequencies where each one of the different mechanisms mainly contributes. Thus, it is possible to construct barriers on demand, and it would also be possible to obtain the maximum category in the standardization test by simply selecting the range of frequencies where the attenuation peaks produced by the different acoustic mechanisms contribute.

With respect to the structural response of the barrier, we have compared the main efforts transmitted to the foundation in both cases, the classical ABs and the one proposed in this work, carrying out a test in a wind tunnel. This is an important structural factor in many cases since the placement of acoustic barriers in certain places is severely restricted by the huge efforts transmitted to the structure where the barrier is located. Thus, as we have demonstrated, the efforts transmitted to the foundations due to the wind are 42% lower in the designed barrier than in the case of the classical ones, usually formed by rigid walls. This reduction allows the use of the SC barrier in situations where until now it was not possible due to structural problems, such as viaducts, where a high classical AB would transmit high efforts to the structure endangering its stability. Nevertheless, more research must be done in this field to obtain definitive conclusions about the use of the SC barriers.

Acknowledgements

This work was supported by MCI Secretaría de Estado de Investigación (Spanish government) and the FEDER funds, under Grant No. MAT2009-09438 and by Universitat Politécnica de Valencia (Programa INNOVA 2010) under grant "INNOVA 2010 PDC PANTALLA ACUSTICA". The authors would like to thank Applus+ (LGAI Technological Center S.A.) and Grupo de Investigación de Dinámica de Flujos Ambientales-Sección Ingeniería de Viento (Universidad de Granada) for their help. V.R.G. is grateful for the support of post-doctoral contracts of the UPV CEI-01-11.

References

Berenger J.P., (1994), A perfectly matched layer for the absorption of electromagnetic waves, *Journal of Computational Physics*, **114**, 185-200.

CEN, (1997a), EN 1793-1. Road Traffic Noise Reducing Devices-Test Method for Determining the Acoustic Performance-Part 1: Intrinsic characteristics of sound absorption, Brussels.

CEN, (1997b), EN 1793-2. Road traffic noise reducing devices-Test method for determining the acoustic performance-Part 2: Intrinsic characteristics of airborne sound insulation under diffuse sound field conditions, Brussels.

CEN, (1997c), EN 1793-3. Road Traffic Noise Reducing Devices-Test method for Determining the Acoustic Performance-Part 3: Normalised Traffic Noise Spectrum, Brussels.

Chen Y.Y., Ye Z., (2001), Theoretical analysis of acoustic stop bands in two-dimensional periodic scattering arrays, *Physical Review E*, **64**, 036616.

EC Directive, (2002), Directive 2002/49/EC of the European Parliament and of the Council of 25 June 2002 relating to the assessment and management of environmental noise, *Official Journal of the European Communities,* **L189**, 12–25.

FHWA U.S.A, (2011), *Keeping the Noise Down. Highway Traffic Noise Barriers*, On line at: http://journalofcommerce.com/Home/News/2007/7/Keeping-the-noise-down---highway-traffic-noise-barriers-JOC023547W/.

Harris C.M., (1991), *Handbook of Acoustical Measurements and Noise Control*, 3rd ed., McGraw-Hill, Inc.

Hu X., Chan C.T., (2005), Two-dimensional sonic crystals with Helmholtz resonators, *Physical Review E*, **71**, 055601.

ISO, (1993), ISO 9613-1:1993 - Acoustics-Attenuation of sound during propagation outdoors-Part 1: Calculation of the absorption of sound by the atmosphere, On line at: http://www.iso.org/iso/catalogue_detail.htm?csnumber=17426

ISO, (1997), ISO 11654:1997 - Acoustics - Sound absorbers for use in buildings - Rating of sound absorption, On line at: https://www.iso.org/obp/ui/#iso:std:iso:11654:ed-1:v1:en.

ISO, (2003), ISO 354:2003 - Acoustics - Measurement of sound absorption in a reverberation room, On line at: http://www.iso.org/iso/iso_catalogue/catalogue_tc/catalogue_detail.htm?csnumber=34545.

ISO, (2010), ISO 10140:2010 - Acoustics-Laboratory measurement of sound insulation of building elements, On line at: http://www.iso.org/iso/iso_catalogue/catalogue_tc/catalogue_detail.htm?csnumber=42089.

John S., (1987), Strong localization of photons in certain disordered dielectric superlattices, *Physical Review Letters*, **58**, 2486-2489.

Kotzen B., English C., (1999), *Environmental Noise Barriers*, E&FN SPON, London.

Kushwaha M.S., Halevi P., Dobrzynski L., Djafari-Rouhani B., (1993), Acoustic band structure of periodic elastic composites, *Physical Review Letters*, **71**, 2022-2025.

Kushwaha M., (1997), Stop-bands for periodic metallic rods: Sculptures that can filter the noise, *Applied Physics Letters*, **70**, 3218-3220.

Lassas M., Somersalo E., (1998), On the existence and convergence of the solution of PML equations, *Computing*, **60**, 228-241.

Liu Q.H., (1999), Perfectly matched layers for elastic waves in cylindrical and spherical coordinates, *Journal of the Acoustical Society of America*, **105**, 2075-2084.

Luo J., Yang Z., (2010), *Research on the Noise Barrier Height Change of the Monocline Viaduct Affecting the Aerodynamic Characteristic of High Speed Train*, Proc. 2010 International Conference on Intelligent Computation Technology and Automation, Changsha (China) 11-12 May 2010, vol. 1, 161.

Maekawa Z., (1968), Noise reduction by screens, *Applied Acoustics*, **1**, 157-173.

Mak C.M., Leung W.S., (2013), Traffic noise measurement and prediction of the barrier effect on traffic noise at different building levels, *Environmental Engineering and Management Journal*, **12**, 449-456.

Martínez-Sala R., Sancho J., Sánchez J.V., Gómez V., Llinares J., Meseguer F., (1995), Sound attenuation by sculpture, *Nature* (London), **378**, 241.

Okubo T., Fujiwara K., (1999), Efficiency of a noise barrier with an acoustically soft cylindrical edge for practical use, *Journal of the Acoustical Society of America*, **105**, 3326-3335.

Platon S.N., Hionis C.A., (2014), Preventing risk of noise exposure in working environment using noise mapping, *Environmental Engineering and Management Journal*, **13**, 1349-1354.

Romero-García V., Sánchez-Pérez J.V., Garcia-Raffi L.M., (2011), Tunable wideband bandstop acoustic filter based on two-dimensional multiphysical phenomena periodic Systems, *Journal of Applied Physics*, **110**, 014904.

Sánchez-Pérez J.V., Caballero D., Martínez-Sala R., Rubio C., Sánchez-Dehesa J., Meseguer F., Llinares J., Gálvez F., (1998), Sound attenuation by a two-dimensional array of rigid cylinders, *Physical Review Letters*, **80**, 5325-5328.

Sánchez-Pérez J.V., Rubio C., Martínez-Sala R., Sánchez-Grandia R., Gómez V., (2002), Acoustic barriers based on periodic arrays of scatterers, *Applied Physics Letters*, **81**, 5240-5242.

Sánchez-Pérez J.V., Martínez-Sala R., Rubio C., Derqui M., (2003), Acoustic Barrier, Spanish Patent, No. *P200200398(X)*

Sánchez-Pérez J.V., Garcia-Raffi L.M., Romero-Garcia V., Castiñeira-Ibáñez S., (2009), Acoustic Barrier, Spanish Patent. No. *P200902074*.

Sigalas M.M., Economou E.N., (1992), Elastic and acoustic wave band structure, *Journal of Sound and Vibration*, **158**, 377-382.

SMD, (2006), Spanish Ministry of Development, Spainsh Technical Building Code, SE-AE Actions in Construction, R.D. 314/2006, *Official Gazette,* March 28, 2006, Madrid, Spain.

Watts G.R., (1996), Acoustic performance of a multiple-edge noise barrier profile at motorway sites, *Applied Acoustics*, **7**, 47-66.

Watts G.R., Morgan P.A., Surgand M., (2004), Assessment of the diffraction efficiency of novel barrier profiles using an MLS-based approach, *Journal of Sound and Vibration*, **274**, 669-683.

Yablonovitch E., (1987), Inhibited Spontaneous Emission in Solid-State Physics and Electronics, *Physical Review Letters*, **58**, 2059-2062.